Structure and Dynamics of Theophylline Derivatives by X-Ray, NMR and Molecular Mechanics Studies

Orenzo Agostini,[a] Graziano Bonacchi,[a] Paolo Dapporto,*[,b] Paola Paoli,[b] Lionello Pogliani[c] and Emilio Toja[a]

[a] *Istituto Farmacobiologico Malesci, S.p.A., Research Center, Firenze, Italy*
[b] *Department of Energetics, University of Firenze, Via S. Marta 3, 50139 Firenze, Italy*
[c] *Department of Chemistry, University of Calabria, Italy*

The two theophylline derivatives 7-isobutyl-1,3-dimethylxanthine (**1**) and 7-butyl-1,3-dimethylxanthine (**2**) show antibronchospastic properties, the first one having a higher pharmacological activity together with a stronger solubility in aqueous solutions. Crystal structures, determined for both compounds, exhibit similar features at the molecular level, but a different crystal packing, *i.e.* compound **2** has a closer arrangement. Melting points and enthalpic data of the two compounds are in agreement with this closer arrangement of compound **2**. NMR measurements show a remarkable mobility of the alkyl side chain of **2** and its very low solubility in aqueous solution. Systematic conformational searches, using the software package provided by Biosym Technologies, were carried out starting from the X-ray crystal structures with the atomic charges calculated with the AM1 routine. Results from these calculations, performed with the CFF91 force field in DISCOVER, underline the high conformational freedom of the side chain of compound **2**. The collected results may be useful to understand the different pharmacological activity between compounds **1** and **2**.

In recent years a great research effort has been made concerning the development of xanthine derivatives having a consistent antibronchospastic activity in a dosage range where they do not produce 'classical' theophylline (1,3-dimethylxanthine) side effects *e.g.* CNS-stimulation and tachycardia.[1,2] 7-Isobutyl-1,3-dimethylxanthine (**1**) which shows a very high pharmacological activity has been already characterized.[3a,b] The isomer, 7-butyl-1,3-dimethylxanthine (**2**), synthesized as already reported,[4] surprisingly shows remarkably lower solubility (in aqueous solution)[5] and activity, notwithstanding the molecular similarity with the above reported derivative **1**—the only difference between the two derivatives being the alkyl side chain which in one case is isobutyl (**1**) and in the other is butyl (**2**).

In this paper we try to shed some light on the noticeably different physicochemical and pharmacological behaviour of the two compounds, comparing (i) their molecular and crystal structure, (ii) their calorimetric data and (iii) their conformational and dynamic behaviour in solution. These studies were accomplished by means of X-ray, calorimetric and NMR measurements and molecular mechanics calculations.

Experimental

Syntheses.—*7-Isobutyl-1,3-dimethylxanthine* **1**. This was prepared as previously described.[3a,b]

7-Butyl-1,3-dimethylxanthine **2**. This was prepared as previously reported.[4]

7-Isobutyl-1,3,8-trimethylxanthine **1**-Me. To a stirred mixture of 72 mg (1.5 mmol) of NaH (50% in paraffin oil) in 4 cm^3 of dimethylformamide (DMF) were added 290 mg (1.5 mmol) of 1,3,8-trimethylxanthine.[6,7] After 30 min, 205 mg (1.5 mmol) of isobutyl bromide were added and the mixture was refluxed for 3 h. The solvent was removed under reduced pressure and the solid residue was taken up with water and filtered to provide 300 mg of a white powder; yield 80% (Calc. for $C_{12}H_{18}N_4O_2$: C, 57.6; H, 7.25; N, 22.4. Found: 57.42; H, 7.11; N, 22.44%).

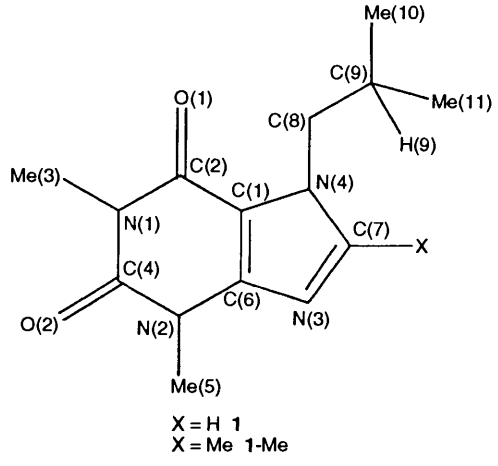

X = H **1**
X = Me **1**-Me

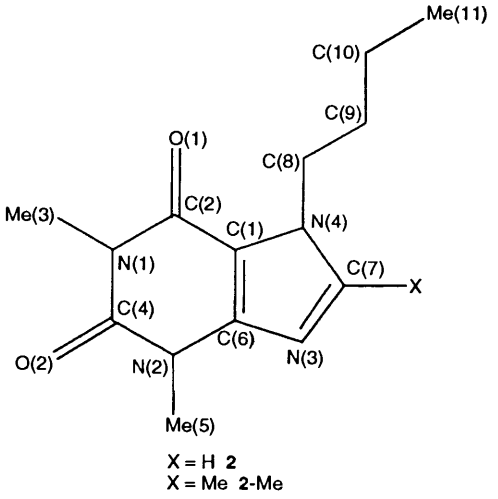

X = H **2**
X = Me **2**-Me

7-Butyl-1,3,8-trimethylxanthine **2**-Me. The method used was identical to that applied for the synthesis of **1**-Me; yield, 80%

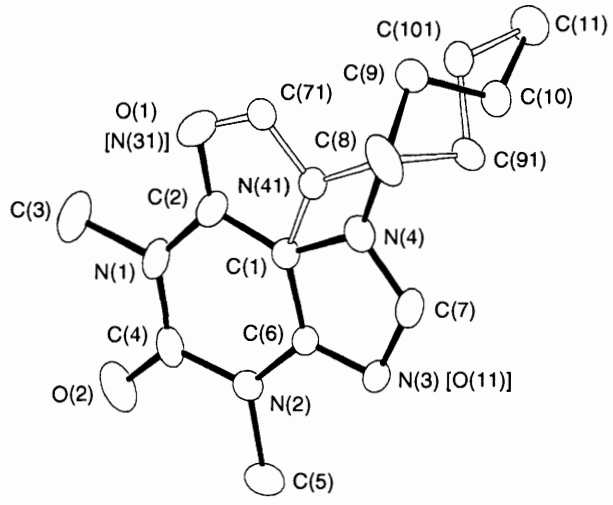

Fig. 1 ORTEP view of compound **2** showing both disordered molecules: **a** (filled bonds) and **b** (unfilled bonds)

(Calc. for $C_{12}H_{18}N_4O_2$: C, 57.6; H, 7.25; N, 22.4. Found: C, 57.46; H, 7.22; N, 22.38%).

The crystal densities of compounds **1**-Me and **2**-Me were obtained from the X-ray determination of the cell parameters.

Crystallography.—Crystal data. $C_{11}H_{16}N_4O_2$ (**2**), M = 236.3. Monoclinic, a = 7.194(1), b = 17.341(4), c = 19.120(7) Å, β = 96.42(2)°, U = 2370(1) Å^3 (by least-squres refinement on diffractometer angles for 25 automatically centred reflections, λ = 1.541 78 Å), space group $C2/c$, Z = 8, D_c = 1.32 g cm^{-3}, $F(000)$ = 1008. Crystal dimensions 0.7 × 0.6 × 0.4 mm, μ(Cu-Kα) = 7.38 cm^{-1}.

Data collection and processing. CAD4 diffractometer, θ–2θ mode, with scan width (1.40 + 0.14 tan θ)°, variable scan speed, graphite-monochromated Cu-Kα radiation; 2292 reflections measured ($2.5 \leq \theta \leq 70°$, h, $+k$, $+l$), 1506 unique with $I > 3\sigma(I)$; absorption with the Walker and Stuart method,[8] calculated minimum and maximum absorption corrections were 0.763 and 1.291 respectively, with the preabsorption R factor of 0.121.

Structure analysis and refinement. Direct methods, SIR88.[9] Full matrix least-squares refinement, weighting scheme $w = 1/[\sigma^2(F_o) + 0.0002\ F_o^2]$. ΔF Fourier showed that the molecule is affected by disorder (see Fig. 1). This disorder, which is accounted for by a non-crystallographic mirror plane passing through O(2), C(4), C(1), C(8) and C(11), allows two distinct positions for the atoms O(1), N(3), N(4), C(7), C(9) and C(10) and for the hydrogen atoms linked to C(7)–C(11). Since the O(1) and N(3) atoms mutually change their positions in the two conformers, their disorder has been neglected in the refinement. Refinement on the population parameters for N(4), C(7), C(9) and C(10) for the two conformers produced values of 0.65 and 0.35 for molecules **a** and **b** respectively. This disordered array continues to exist also if the acentric Cc space group is considered, so confirming the $C2/c$ space group as the correct one. Hydrogen atoms were introduced in calculated positions and refined accordingly to the linked carbon atoms, with an overall isotropic temperature factor U of 0.08 Å^2. Anisotropic thermal parameters were used for non-hydrogen atoms. A Fourier difference map performed in the last refinement cycle did not show any interesting features, the highest peak being 0.21 e Å^{-3}. The final R factor was 0.068, whereas the R_w factor was 0.079. All calculations were performed with the SHELX-76[10] set of programs which use the analytical approximation for the atomic scattering factors and anomalous dispersion corrections for all the atoms from the *International Tables of X-Ray Crystallography*.[11]

Table 1 Dihedral angles (°) of the conformers found from the conformational search for **1** and **2**

Conformer	φ_1	φ_2	φ_3	Conformation
Compound **1**				
1	102.2	50.1		*gg*
2	83.7	−49.9		*gg*
3	99.9	178.4		*gt*
Compound **2**				
1	86.7	179.4	179.4	*gtt*
2	86.0	178.6	70.6	*gtg*
3	82.8	71.5	178.5	*ggt*
4	101.3	−70.6	177.9	*gg*$^-$*t*
5	86.9	178.6	−71.2	*gtg*$^-$
6	84.2	68.5	67.6	*ggg*
7	107.5	−69.7	−72.2	*gg*$^-$*g*$^-$
8	111.3	−76.4	83.2	*gg*$^-$*g*
9	78.0	75.2	−85.8	*ggg*$^-$

Tables of thermal parameters, atomic coordinates, bond distances and angles have been deposited at the Cambridge Crystallographic Data Centre.*

Calorimetric Measurements.—Calorimetric measurements were carried out on compounds **1**, **2** and their 8-methyl-substituted derivatives. The thermal curves were evaluated by means of a Perkin-Elmer (PE) DSC 7 power compensation differential scanning calorimeter equipped with PE pc software and used in the non-isothermal mode, with a dry nitrogen flow of 16 cm^3 min^{-1} purging the apparatus cell. The scanning rate employed was 5 °C min^{-1}.

NMR Measurements.—Solutions of compound **1** and **2** in $CDCl_3$ were 1 mol dm^{-3}, while solutions in D_2O were *ca.* 0.10 and 0.01 mol dm^{-3} respectively (saturated solutions). NMR spectra were recorded at 20 °C on a Bruker AC-300 NMR spectrometer. For the T_1 (^{13}C) measurements the duration of the 90° pulse was 8.5 μs (5 mm probe) and the delay time was 100 s. T_1 values are the mean of three different measurements. The $CHCl_3$ peak positioned at 7.26 ppm (proton spectra) and the $CDCl_3$ central peak at 77 ppm were used as internal standards. Eight and 512 scans were accumulated to obtain the ^{1}H spectra in water of **1** and **2** respectively. The water peak positioned at 4.8 ppm was used as the internal standard. The error is estimated to be within 0.01 ppm, 0.05 ppm and 0.2 Hz for proton, carbon chemical shifts and proton coupling constants respectively. T_1 relaxation times are 12% accurate.

Theoretical Calculations.—The atomic charges of compounds **1** and **2**, starting from their experimental geometries, were calculated with semi-empirical molecular orbital calculations by using the AM1 method of the MOPAC package, version 6.0.[12]

Conformational analyses employing X-ray structures as starting points were carried out on the two molecules to explore the range 0–360° for the isobutyl and butyl side chains. The torsion angles involved were C(1)–N(4)–C(8)–C(9) (φ_1^1) and N(4)–C(8)–C(9)–H(9) (φ_2^1) for the isobutyl derivative, with rotation steps of 15°, while for the butyl substituent they were C(1)–N(4)–C(8)–C(9) (φ_1^2), N(4)–C(8)–C(9)–C(10) (φ_2^2) and C(8)–C(9)–C(10)–C(11) (φ_3^2) by using angular increments of 30°. Table 1 reports the angular values of the dihedral angles for

* For details of the CCDC deposition scheme, see 'Instructions for Authors (1994),' *J. Chem. Soc., Perkin Trans. 2*, 1994, issue 1.

each conformer of **1** and **2** found by the aid of the following minimization procedures: steepest descents, conjugate gradient and quasi-Newton–Raphson methods. The force field used was CFF91 provided by DISCOVER.[13] These computational results were obtained by using the software programs of Biosym Technologies, San Diego: INSIGHTII, DISCOVER, SEARCH-COMPARE and ANALYSIS.

All calculations were performed on an IBM RISC/6000 computer, model 320H.

Results and Discussion

Description of the Structure.—An ORTEP[14] drawing of the disordered molecules is shown in Fig. 1. Fig. 2 is a view of the molecular packing of compounds **1** and **2**. Table 2 lists bond distances and angles. Table 3 reports the conformation of the butyl chain in the two disordered molecules together with the conformation of the isobutyl chain in compound **1**. The angle between the mean square plane of the two rings and the mean square line passing through the four carbon atoms of the butyl chain is near to perpendicular, being 74.6(1)° and 73.5(3)° for molecules **a** and **b** respectively. The packing drawing [Fig. 2(*b*)] shows that the molecules lie almost parallel to each other, the angles between the planes of the two rings being 4.38(7)°, thus allowing a very compact arrangement of the molecules, with the butyl chains pointing to the interspace of the molecular rings. This packing appears to be stabilized by 'graphite-like' interactions between molecules lying each one above the other. The drawing has been constructed with the molecule **a**, due to the impossibility (because of the disorder of introducing in the right positions) the **b** one. This representation, on the other hand, cannot be noticeably influenced by this disordered array, because the two molecules superimpose in all the non-hydrogen atoms of the two rings, except in N(4) and C(7). It is evident, comparing this packing with that of the analogous isobutyl derivative [Fig. 2(*a*)], where the molecules lie on two different planes (the relative angle is 42.0°), that in the butyl derivative the molecular packing is more compact. As a matter of fact the calculated density differs by about 5% in the two compounds (1.26 *vs.* 1.32 g cm^{-3} for **1** and **2**, respectively). The intermolecular interactions of the hydrogen in the eighth position, H(7), with the oxygen atoms of the carbonyl groups in both disordered molecules [H(7)···O(2) = 2.356(6) and H(71)···O(1) or N(31) = 2.30(1) Å] seems to be rather interesting. In compound **1** an analogous but significantly weaker interaction was found [H(7)···O(2) equal to 2.60 Å]. Also the directions of the hydrogen bonds attest that they are stronger in compound **2**, the angles being C(7)–H(7)···O(2) 169.7(7), C(71)–H(71)···O(1) 175(1)° in **2**, against a value of 141° for C(7)–H(7)···O(2) in **1**.

In conclusion the higher density of compound **2** can be justified by considering (i) the 'graphite-like' interactions between molecular rings and (ii) the stronger hydrogen bond involving molecules lying on the same plane.

Calorimetric Data.—In order to quantify, from an energetic point of view, the difference in the solid state interactions of compounds **1** and **2** and to test the role played by the hydrogen atom in the 8-position, a calorimetric study has been undertaken on **1**, **2** and their 8-methyl derivatives (**1**-Me, **2**-Me). Table 4 collects calorimetric data together with the water solubility and the calculated density for the four molecules. The values obtained for the melting enthalpy of compounds **1** and **2** agree well with the corresponding calculated density, *i.e.*, the higher enthalpy is related to the larger density, thus to a closer crystal packing as stated before. The similar ΔH values of **1**-Me and **2**-Me seem to confirm that the intermolecular interaction involving the hydrogen in the eighth position is mainly

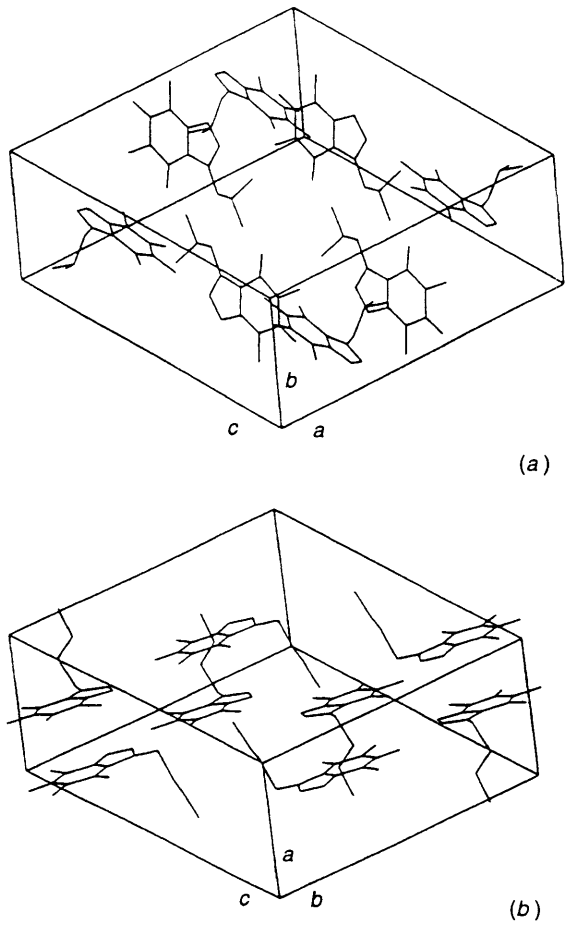

Fig. 2 Packing diagram of: (*a*) compound **1** [ref. 3(*a*)] and (*b*) compound **2**

Table 2 Bond distances (Å) and angles (°) for the butyl derivative, esds in parentheses

N(31)–C(71)	1.25(1)	N(4)–C(7)	1.354(9)
O(1)–C(2)	1.278(6)	N(4)–C(1)	1.432(6)
O(2)–C(4)	1.205(5)	N(4)–C(8)	1.343(8)
N(1)–C(2)	1.393(5)	N(41)–C(71)	1.30(1)
N(1)–C(3)	1.466(6)	N(41)–C(1)	1.34(1)
N(1)–C(4)	1.388(6)	N(41)–C(8)	1.39(1)
N(2)–C(4)	1.385(5)	C(1)–C(2)	1.386(5)
N(2)–C(5)	1.467(4)	C(1)–C(6)	1.380(6)
N(2)–C(6)	1.390(5)	C(8)–C(9)	1.607(9)
N(3)–C(7)	1.338(7)	C(9)–C(10)	1.50(1)
N(3)–C(6)	1.297(5)	C(10)–C(11)	1.475(9)
C(8)–C(91)	1.65(1)	C(91)–C(101)	1.52(2)
C(101)–C(11)	1.48(1)		
C(71)–N(31)–C(2)	100.3(6)	N(41)–C(1)–C(2)	92.4(5)
C(3)–N(1)–C(4)	116.3(4)	N(4)–C(1)–C(6)	99.7(4)
C(2)–N(1)–C(4)	124.6(3)	N(4)–C(1)–C(2)	136.6(4)
C(2)–N(1)–C(3)	119.1(4)	C(2)–C(1)–C(6)	123.7(3)
C(5)–N(2)–C(6)	119.6(3)	N(1)–C(2)–C(1)	115.2(3)
C(4)–N(2)–C(6)	122.3(3)	O(1)–C(2)–C(1)	121.1(3)
C(4)–N(2)–C(5)	118.1(3)	O(1)–C(2)–N(1)	123.7(4)
C(7)–N(3)–C(6)	101.6(4)	N(1)–C(4)–N(2)	116.4(3)
C(1)–N(4)–C(8)	133.0(5)	O(2)–C(4)–N(2)	121.8(4)
C(7)–N(4)–C(8)	120.8(6)	O(2)–C(4)–N(1)	121.7(4)
C(7)–N(4)–C(1)	106.1(5)	N(3)–C(6)–C(1)	118.6(3)
N(3)–C(7)–N(4)	114.0(5)	N(2)–C(6)–C(1)	117.8(3)
C(1)–N(41)–C(8)	138.0(8)	N(2)–C(6)–N(3)	123.7(3)
C(71)–N(41)–C(8)	107.7(9)	N(41)–C(8)–C(91)	107.9(6)
C(71)–N(41)–C(1)	114.3(9)	N(4)–C(8)–C(9)	114.6(5)
N(31)–C(71)–N(41)	112(1)	C(8)–C(9)–C(10)	107.8(5)
N(41)–C(1)–C(6)	143.9(5)	C(9)–C(10)–C(11)	113.3(6)
C(8)–C(91)–C(101)	101.6(8)	C(91)–C(101)–C(11)	117(1)

Table 3 Dihedral angles (°) for **1** [ref. 3(*a*)] and **2**, as found from the X-ray analysis, esds in parentheses

Compound **1**			
C(1)–N(4)–C(8)–C(9)	73		
N(4)–C(8)–C(9)–H(9)	−55		
Compound **2**	molecule **a**		molecule **b**
C(1)–N(4)–C(8)–C(9)	−70.6(7)	C(1)–N(41)–C(8)–C(91)	66.2(12)
N(4)–C(8)–C(9)–C(10)	−69.9(7)	N(41)–C(8)–C(91)–C(101)	82.6(9)
C(8)–C(9)–C(10)–C(11)	−179.0(5)	C(8)–C(91)–C(101)–C(11)	174.1(8)

Table 4 Calorimetric, melting point, solubility and calculated density values for **1**, **2**, **1**-Me and **2**-Me

Compound	M.p./°C	ΔH/kcal mol^{-1} [a]	ΔS/cal K^{-1} mol^{-1} [a]	ρ_{20}/g cm^{-3}	s_{20}/g dm^{-3} [b]
1	90.9	4.49	12.34	1.26	27
2	105.1	7.23	19.11	1.32	3.7
1-Me	134.6	6.10	14.96	1.29	6.3
2-Me	127.7	6.65	16.59	1.28	4.5

[a] Melting. [b] Water solubility.

responsible for determining the very different values in the melting enthalpy for **1** and **2**, rather than the alkyl side chain. Furthermore the higher values for the entropy change, which are associated with the butyl compounds **2** and **2**-Me, can be related to the larger conformational freedom that can be reached by the butyl chain in the liquid state in comparison of that of the isobutyl one. On the other hand molecule **2**, also in the solid state, should have a larger entropic content, as evidenced by the disordered array found in the crystal structure, but, nevertheless, the melting brings a bigger entropic increase. On the basis of these results we could explain the surprising differences in the water solubility for **1** and **2** as due to the different reticular energy between the two molecules. Because the substitution of the H(7) atom in both compounds with a methyl group causes the solubilities of both derivatives to become nearly identical, we can infer the importance of the hydrogen bond found in the crystal structure of **2**.

NMR Measurements.—^{1}H and ^{13}C NMR data have been collected in Tables 5 and 6 respectively. Due to the very low solubility of **2** in water it was not possible to obtain ^{13}C NMR spectra of this compound in aqueous media. Anyway, analysis of the obtained NMR data gives us some interesting hints about structure and dynamics of these two compounds in chloroform and in aqueous solutions.

Proton data. The vicinal coupling constants, ^3J, of compounds **1** and **2** in water and chloroform show that they are typical of freely rotating ethane fragments.[15,16] The proton chemical shifts of compounds **1** and **2** in chloroform are very similar (within the given error limits); in aqueous solutions δ[H(5)] and δ[H(3)] are different in the two compounds (nearly −0.08 and −0.07 ppm, respectively). The high-field shift of H(5)(**1**) and H(3)(**1**) could be caused by a small out-of-plane deviation (plane of the π-electrons)[15,16] of the methyl groups in **1**. A similar explanation could be valid for the chemical shift differences of the side-chain endings in **1** and **2**: in water, in fact, δ[H(10,11)](**1**) and δ[H(11)](**2**) differ by *ca.* −0.06 ppm. The constancy of the chemical shift difference between H(7)(**1**) and H(7)(**2**) in the two solvents is mainly caused by a dominant paramagnetic shift due to the nearby in-plane π-electron system.[15,16]

Carbon data. Analysis of the carbon chemical shifts in chloroform shows the striking similarities of the carbon shifts of the xanthine system of compounds **1** and **2** and the similar chemical shift between C(10,11)(**1**) and C(10)(**2**). Of note is the particular proton and carbon shift sequence, from low to high

Table 5 ^{1}H NMR parameters of compounds **1** and **2** in chloroform and water (primed values)[a]

Assignments	δ	δ'	^3J/Hz	$^3J'$/Hz
H(10,11) **1**	0.864	0.838	6.8	6.8
H(11) **2**	0.874	0.893	7.3	7.3
H(10) **2**	1.270	1.279	7.4	7.4
H(9) **2**	1.781	1.798	7.3	7.2
H(9) **1**	2.152	2.021	7.0	6.9
H(8) **1**	4.011	4.023	7.2	7.1
H(8) **2**	4.218	4.287	7.1	7.1
H(5) **1**	3.326	3.251		
H(5) **2**	3.321	3.330		
H(3) **1**	3.515	3.446		
H(3) **2**	3.507	3.514		
H(7) **1** [b]	7.464	7.937		
H(7) **2** [b]	7.493	7.965		

[a] Labelling corresponds to bound carbon atoms. [b] Xanthine ring proton.

Table 6 ^{13}C NMR parameters of compounds **1** and **2** in chloroform

Assignments	δ(**1**)	δ(**2**)	NT_1(**1**) [a]/s	NT_1(**2**)/s
C(11)	19.18	12.99	3.6	9.3
C(10)	19.18	19.09	3.6	4.2
C(9)	29.23	32.40	1.6	2.8
C(8)	53.88	46.47	1.6	1.5
C(5)[c]	27.49	27.40	11.4	12.0
C(3)[c]	29.28	29.18	11.7	12.6
$C(1)_q$ [b,c]	106.65	106.44	13.4	14.4
C(7)[c]	140.97	140.51	1.2	1.1
$C(6)_q$ [c]	148.51	148.45	13.1	11.8
$C(4)_q$ [c]	151.22	151.16	12.2	10.7
$C(2)_q$ [c]	154.22	154.56	11.5	9.2

[a] N is the number of protons directly bound to carbon atoms. [b] q, quaternary carbons: in this case $NT_1 = T_1$. [c] Xanthine ring carbon.

frequencies, at positions 8 and 9 along the two compounds in chloroform (in water this is valid only for proton shifts): H(9)(**2**), H(9)(**1**), H(8)(**1**), H(8)(**2**) and C(9)(**1**), C(9)(**2**), C(8)(**2**), C(8)(**1**). This back-to-back pattern[17,18] might be used as a tool in the assignment of xanthine derivatives in solution. Analysis of carbon longitudinal relaxation times in chloroform (see Table 6) shows the growing mobility, expressed by the growing T_1 values[19] of the butyl side-chain of compound **2**. Due to the detected similarities between **2** in water and chloroform, we

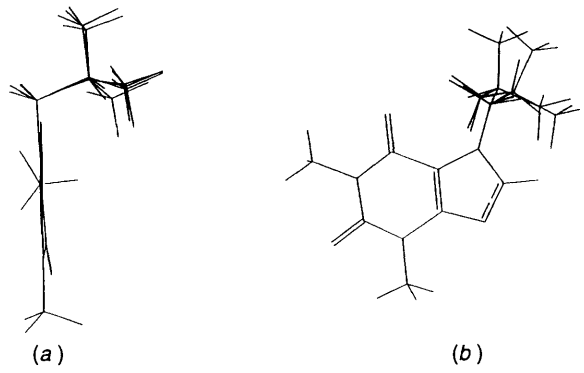

Fig. 3 Superposition of the conformers for the isobutyl derivative: (*a*) side view; (*b*) front view

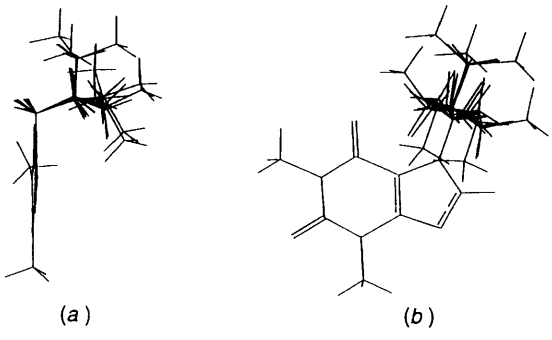

Fig. 4 Superposition of the conformers for the butyl derivative: (*a*) side view; (*b*) front view

can assume that the growing mobility of the butyl side-chain should be retained in aqueous solutions. With the assumption that relaxation in protonated carbons is dominated by the dipole–dipole mechanism and that molecules **1** and **2** are tumbling isotropically and fast in solution, it is possible to estimate,[19] by the aid of T_1[C(7)], the correlation τ_0 time for the overall molecular motion of **1** and **2** in chloroform, which is equal to *ca.* 43 ps. The higher mobility of the hydrophobic side-chain of **2** might have a destabilizing effect on the solute–solvent interactions in aqueous medium, with resulting poorer solubility of compound **2** in water.

Theoretical Calculations.—No significant difference was noticed in the atomic charges of **1** and **2**, either in the alkyl side chain or in the 1,3-dimethylxanthine ring.

Results from the conformational analysis show, with respect to the different steric hindrance of the two alkyl chains, that for the butyl derivative a larger number of conformers is available than for the isobutyl one, being 6 and 18, for **1** and **2** respectively. Because of their symmetrical disposition in respect to the rings' plane only three and nine conformers were considered (see Table 2, Figs. 3 and 4). The energies of the three conformational isomers for the isobutyl derivative are comprised within 2.7 kcal mol^{-1}, while the energy content of the nine conformers found for the butyl isomer differs up to a maximum of 3.7 kcal mol^{-1}. It is noteworthy that the conformation displayed by the dihedral angle φ_1 is similar in all the conformers found for both compounds (see Table 2) and in satisfactory agreement with the experimental angular value. To evaluate the energy barriers for the interconversion between the nine conformers of the butyl derivative two two-dimensional energy maps of the dihedral angles $\varphi_2{}^2$ and $\varphi_3{}^2$ were obtained, by keeping the $\varphi_1{}^2$ at 84° and 107°, respectively. Fig. 5 reports the energy map for $\varphi_1{}^2 = 84°$. In both cases the maximum barrier to overcome for the conformer interconversion is about

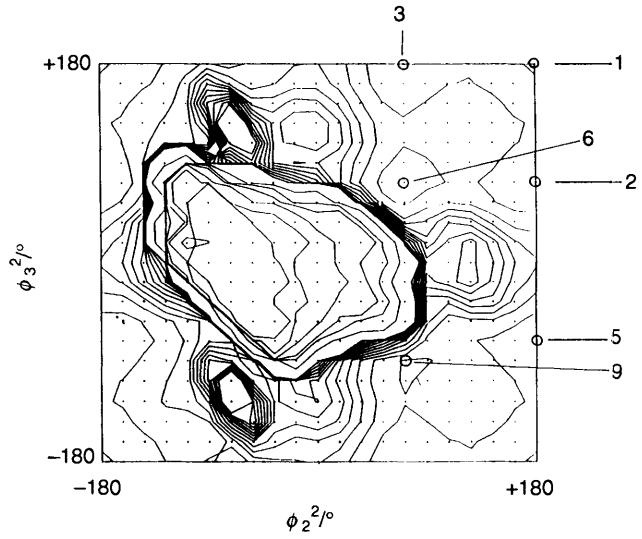

Fig. 5 Two-dimensional energy map of the butyl derivative as a function of the two dihedral angles $\varphi_2{}^2$ and $\varphi_3{}^2$ obtained by keeping the $\varphi_1{}^2$ angle fixed at 84°. The energy is contoured in 4 kcal mol^{-1} intervals up to a value of 50 000 kcal mol^{-1}. The locations numbered correspond to the conformers listed in Table 2. The isomers 4, 7 and 8 are not located in a minimum, owing to their different $\varphi_1{}^2$ angles (see Table 2); however in the analogous study performed at $\varphi_1{}^2 = 107°$ they lie in well defined minima.

10 kcal mol^{-1}. A nearly identical torsional barrier was found for the rotation around the $\varphi_2{}^2$ angle in the isobutyl derivative. Therefore, whereas the butyl and isobutyl side chains are rather rigid with regard to the dihedral angle φ_1, we can postulate a considerable conformational freedom for the rest of the alkyl chain in both molecules. This result agrees well with the experimental evidence from the NMR studies.

All collected data indicate that the different physico-chemical behaviour of molecules **1** and **2** is mainly due to the following parameters: (*a*) the diversity in the reticular energy of the two isomers because of the interaction *via* a hydrogen bond, involving H(7) of **2**; and (*b*) their different conformational freedom as provided by NMR and theoretical studies.

These results could constitute a preliminary approach to a structure–activity study on theophylline-derived drugs.

References

1 S. Snyder and P. J. Sklar, *Psychiatr. Res.*, 1984, **18**, 91.
2 C. G. A. Persson, *J. Allergy Clin. Immunol.*, 1986, **78**, 780.
3 (*a*) O. Agostini, G. Bonacchi, P. Dapporto, P. Paoli, M. Fedi and S. Manzini, *Arzneim.-Forsch./Drug Res.*, 1990, **40**, 1089; (*b*) M. Fedi and G. Bonacchi, Patentschrift DE 3328636C2, 1991.
4 D. Guttman and T. Higuchi, *J. Am. Pharm. Assoc.*, 1957, **46**, 10.
5 S. Bolton, D. Guttman and T. Higuchi, *J. Am. Pharm. Assoc.*, 1957, **46**, 38.
6 J. H. Speer and A. L. Raymond, *J. Am. Chem. Soc.*, 1953, **75**, 114.
7 H. Bredereck, I. Hennig, W. Pfleiderer and G. Weber, *Chem. Ber.*, 1953, **86**, 333.
8 N. Walker and D. D. Stuart, *Acta Crystallogr., Sect. A*, 1983, **39**, 158.
9 M. C. Burla, M. Camalli, G. Cascarano, C. Giacovazzo, G. Polidori, R. Spagna and D. Viterbo, *J. Appl. Crystallogr.*, 1989, **22**, 389.
10 G. M. Sheldrick, SHELX 76, *A Program for Crystal Structure Determination*, University of Cambridge, UK, 1976.
11 *International Tables for X-Ray Crystallography*, Kynoch Press, Birmingham, 1974, vol. 4.
12 J. J. P. Stewart, *QCPE*, Program No. 455.
13 Biosym Technologies, Inc., 9685 Scranton Road, San Diego, CA 92121-2777.

14 C. K. Johnson, ORTEP, Report ORNL 3794, Oak Ridge National Laboratory, TN, 1971.
15 H. Günther, *NMR Spectroscopy, An Introduction*, Wiley, New York, 1980.
16 R. K. Harris, *Nuclear Magnetic Resonance Spectroscopy. A Physicochemical View*, Pitman, London, 1983.
17 D. E. Dorman and F. A. Bovey, *J. Org. Chem.*, 1973, **38**, 1719.
18 L. Pogliani, M. Ellenberger, J. Valat and A. M. Bellocq, *Int. J. Peptide Protein Res.*, 1975, **7**, 245.
19 J. R. Lyerla, Jr., H. M. McIntyre and D. A. Torchia, *Macromolecules*, 1974, **7**, 11.

Paper 3/06667C
Received 8*th November* 1993
Accepted 11*th January* 1994